PAPER

Check for updates

Cucurbit[10]uril binding of heteroleptic iridium(III) complexes: synthesis and photophysical characterization

Lubna Alrawashdeh, [iD] *[a] Shrouq Almarabeh,[a] Khaleel I. Assaf, [iD] *[b] Anthony I. Day, [iD] [c] Lynne Wallace [iD] [c] and Suhair A. Bani-Atta [iD] [d]

The supramolecular host–guest interaction between heteroleptic iridium(III) complexes and cucurbit[10]uril (Q[10]) in an aqueous medium was investigated in this work. Both studied iridium complexes, $[Ir(ppy)_2(bpy-(CHO)_2)]^+$ (complex **1**) and $[Ir(ppy)_2(bpy-(COOH)_2)]^+$ (complex **2**), possessed two phenylpyridine ligands and a single R-bipyridine ligand. The formation of the encapsulated species (Q[10]·**1** and Q[10]·**2**) was demonstrated by ^1H NMR and luminescence studies. A significant improvement was observed in the luminescence properties of both iridium complexes (emission intensity, quantum yield and lifetime) upon the addition of Q[10] in an aqueous medium. Results suggested a major effect of the hydrophobic cavity in the destabilization of the ^3MLCT state (lowest excited state) of the iridium complexes. The binding study of both complexes with Q[10] revealed the formation of 1:1 and 1:2 host–guest species, with the binary complex dominating the emission behavior. The equilibrium between the emitting species was significantly influenced by the temperature, wherein the 1:1 inclusion complex was less favorable at elevated temperatures. The effect of pH on the emission profiles of the free and encapsulated iridium complexes was also investigated in this study. Density functional theory (DFT) calculations showed that introducing different substituent groups (CHO and COOH) on the bpy ligand had a negligible effect on the orientation of these complexes within the Q[10] cavity.

Introduction

Luminescent transition-metal complexes have attracted significant research interest due to their wide range of applications. Among them, cyclometalated iridium(III) complexes are considered one of the best luminescent materials due to their distinctive photophysical properties, such as photostability, high quantum yield, and extremely tunable optoelectronic properties.[1] Thus, they have a range of applications in the areas of organic light-emitting diodes (OLEDs),[2] light-emitting electrochemical cells (LECs),[3] and in catalysis.[4,5] Distinct focus has been given to using cyclometalated iridium(III) complexes as chemosensors for a variety of analytes, such as ions,[6] gaseous species,[7] and biomolecules,[8,9] due to the sensitivity of their emitting state to the local environment. Thus, tuning the emission can be achieved by changing the attached ligands,

adding different substituent groups on the ligands, or even by changing the solvent. These changes can directly affect the HOMO–LUMO gap, which is reflected in changes found in the emission wavelength.[10] For most cyclometalated iridium complexes, the triplet metal-to-ligand charge-transfer (^3MLCT) state is the lowest excited state, and it is responsible for the emission properties.[11]

Previous studies have shown that several cyclometalated iridium(III) complexes have serious limitations as sensors for biological analytes because of their poor water solubility and weak emission intensity in aqueous media.[12,13] Based on this, various studies have been undertaken to develop water-soluble luminescent cyclometalated iridium(III) complexes by changing the attached substituent groups (more hydrophilic) on the ligands.[14,15] Recently, our group proposed a novel method to overcome the limitations by changing the environment around iridium complexes. This was obtained by applying host–guest chemistry to selected metal complexes using cucurbit[*n*]urils (Q[*n*]) as host molecules. The aqueous solubility and emission properties were significantly improved after encapsulating the iridium complexes within the hydrophobic cavity of Q[*n*].[16]

Q[*n*] are a prominent family of water-soluble macrocyclic host molecules that have garnered considerable attention in the field of supramolecular host–guest chemistry.[17,18] They consist of *n* glycoluril units (*n* = 5–8, 10) connected by methylene

[a]Department of Chemistry, Faculty of Science, The Hashemite University, P.O. Box 330127, Zarqa 13133, Jordan. E-mail: lubna.reyad@hu.edu.jo; shrouqalmarabeh@gmail.com

[b]Department of Chemistry, Faculty of Science, Al-Balqa Applied University, Al-Salt 19117, Jordan. E-mail: khaleel.assaf@bau.edu.jo

[c]School of Physical, Environmental and Mathematical Sciences, UNSW Australia, Australian Defence Force Academy, Canberra, Australia. E-mail: a.day@unsw.edu.au; lynne.wallace@unsw.edu.au

[d]Analytical Chemistry Research Laboratory, Department of Chemistry, Faculty of Science, University of Tabuk, Tabuk 71491, Saudi Arabia. E-mail: s_bantatta@ut.edu.sa

bridges and have portal dimensions of 2.4–11.0 Å.[17] Q[n] are pumpkin-shaped, highly symmetrical macrocycles with a hydrophobic cavity suitable for accommodating neutral/non-polar guest molecules,[19] and carbonyl rims offer binding sites for non-covalent interactions (such as hydrogen bond and ion–dipole interactions).[20] Q[n] have advantages over other host molecules such as cyclodextrins and calixarenes because of their high selectivity[21] and affinity[20] toward guest molecules. Q[n] have been used in many applications, including sensing,[22] separation,[23] molecular recognition,[24] drug delivery and biomedical systems.[25–27]

Q[10] is the member that possesses the largest accessible cavity (870 Å³ and portal diameter = 11 Å) among the commonly used members of the family (Q[5]–Q[10]).[28] Recently, larger Q[n] homologues (n = 13–15) have also been isolated; however, their "twisted" conformations limit the available space in the cavity.[29,30] Thus, Q[10] can encapsulate large-sized guests or two small guest molecules to form ternary complexes.[31,32] Moreover, special attention has been given to encapsulating large transition metal complexes for various applications. For example, Q[10] has been used as a drug vehicle for di-ruthenium and di-platinum complexes,[33] while various encapsulated mono-ruthenium complexes within the Q[10] cavity have been investigated to study the formation of supramolecular photocatalyst systems.[34] Wallace and coworkers showed that large tris–chelate transition metals (Ru and Ir) can also be accommodated within the Q[10] host molecule.[35]

Many studies have demonstrated that Q[n] can be used to tune the photophysical properties of luminescent dyes;[36] based on this point, we previously applied host–guest chemistry to some large luminescent cyclometalated iridium(III) complexes. Sizable enhancement in the luminescence properties and aqueous solubility of these complexes was obtained upon encapsulation inside Q[10].[16,37] Wallace showed that this effect is not universal for all iridium complexes and depends mainly on the electronic structure of the guest.[35] Herein, we extend our previous work to consider more polypyridyl iridium(III) complexes with different electronic properties. These complexes have different substituent groups on the bpy ligand ([Ir(ppy)₂(bpy-R)]^{n+}) and are commonly used in sensing applications. In addition, the effect of changing the position of the substituent groups on the binding mode, luminescence and solubility properties of these complexes will be explored. Aldehyde (–CHO) and carboxylic acid (–COOH) moieties are used as

substituent (R) groups in this study (Fig. 1) because of their benefits as building blocks in the synthesis of sensors.[38,39] Furthermore, the ionizable nature of the carboxylic acid group enables pH-dependent behavior, which is valuable for designing pH-sensitive sensors and systems that respond to biological environments.

Experimental

Materials and instruments

Iridium(III) chloride hydrate, 2,2′-bipyridine-4,4′-dicarboxylic acid, 2,2′-bipyridine-4,4′-dicarboxyaldehyde, 2-phenylpyridine, tris(2,2′-bipyridyl)ruthenium(II) chloride ([Ru(bpy)₃]Cl₂), NH₄PF₆, 2-ethoxy ethanol, and sodium acetate (anhydrous) were obtained from Sigma-Aldrich (USA). Methanol, HCl, toluene, hexane, acetone and tert-butanol (t-BuOH) were obtained from Tedia (USA). Glacial acetic acid was purchased from Fisher Chemical. Acetonitrile and dichloromethane were obtained from Anaqua Chemical Supply (ACS). Q[10] and Q[8] were prepared by Anthony Day (UNSW/Australia), according to the method described in the literature.[40,41] For NMR experiments, all deuterated solvents and deuterated acetic acid were purchased from Sigma-Aldrich, and sodium acetate buffer (0.05 M, pH = 4.7) was prepared from solid sodium acetate and deuterated acetic acid dissolved in D₂O.

¹H NMR spectra were recorded using a Bruker AVANCE-III 400 MHz NanoBay FT-NMR spectrometer at 25 °C, and tetramethylsilane (TMS) was used as a reference. Luminescence spectra were recorded using a Jasco spectrofluorometer (FP-6500). This spectrofluorometer was also used to study the temperature dependence of the emission spectra, and a circulating water bath (Jeio Tech RW-1025G) was used for controlling the temperature. Samples were excited at 350 nm using quartz cuvettes (1 cm path length). Luminescence lifetimes were determined using a spectrofluorometer from Edinburgh Analytical Instruments FL-900S (Germany) equipped with time-correlated single photon counting. Sample decay was fitted using exponential tail fit analysis. The value of the χ² was used to assess the quality of the fitted result (which should be close to 1.00 for a successful fit). UV-visible spectra were recorded on a Cary 100 UV-Visible spectrophotometer. Acetate buffer (0.05 M, pH = 4.7) was used to calculate the absorption coefficients (ε) of the iridium complexes.

Quantum yields were measured in acetate buffer at an excitation wavelength of 350 nm. The optically dilute method with single-point measurements was used for this purpose.[42] A deaerated [Ru(bpy)₃]²⁺ aqueous solution was used as a reference (λ_ex = 350 nm, Φ_R = 0.042). In this method, the quantum yield was found based on eqn (1):

$$\Phi_x = \Phi_R [I_X/I_R][A_R/A_x][\eta_x^2/\eta_R^2] \qquad (1)$$

Φ_x and Φ_R are the quantum yields of the unknown and reference, respectively; I_x and I_R are the integrated emission intensities of our sample and reference, respectively; A_x and A_R are the absorbance of our sample and reference at the excitation wavelength, respectively; and η_x and η_R are the refractive indices
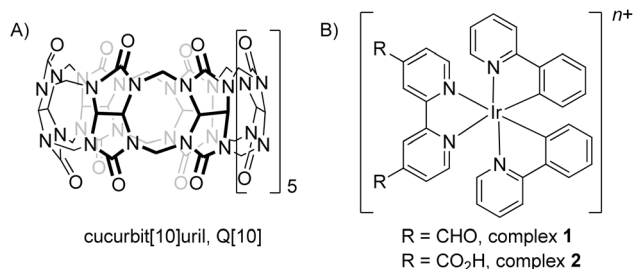

Fig. 1 Chemical structures of (A) Q[10] and (B) iridium(III) cyclometalated complexes.

cucurbit[10]uril, Q[10]

R = CHO, complex 1
R = CO₂H, complex 2

of the solvents. The refractive index of acetate buffer (solvent) is 1.34.[43]

^{1}H NMR spectroscopy of host–guest complexes

In the preliminary ^{1}H NMR experiments (400 MHz, D$_2$O/acetate-d_4 buffer), solid Q[10] was added directly to the individual solutions of guests **1** and **2**. The addition of the macrocycle immediately produced a visible precipitate, implying that the resulting inclusion complexes were substantially less soluble in water than either the free host or the free guests. To obtain reliable spectroscopic data on these low-solubility adducts, the measurements were conducted on a higher-field instrument (500 MHz), followed by optimisation of the acquisition parameters (see the SI for details).

Determination of the Q[10] concentration by ^{1}H NMR spectroscopy

The Q[10] concentration in acetate buffer was determined by adding 5 μL of a standard solution of *t*-BuOH (0.01 M) to the Q[10] NMR sample of known volume (prepared by dissolving a certain amount in acetate buffer, sonication, and centrifugation to obtain a clear dissolved sample). The integration value of Q[10] proton peaks was compared to that of the standard *t*-BuOH peak in order to determine the concentration of Q[10].

Photophysical study

In the photophysical study, iridium complexes and Q[10] solutions were prepared in acetate buffer (0.05 M, pH 4.7). For absorption titration experiments, various amounts of the Q[10] stock solution (2.0×10^{-5} M) were added to 2.5 mL of the solution of complex **1** (5.9×10^{-6} M) or complex **2** (7.6×10^{-7} M). For luminescence titration experiments, different amounts of the Q[10] stock solution (2.0×10^{-5} M) were added to 2.5 mL of the solution of complex **1** (5.9×10^{-6} M) or complex **2** (7.6×10^{-7} M). For the luminescence study of Q[8] with iridium complexes, an excess solid of Q[8] was added to both iridium complexes in acetate buffer to form saturated samples. Centrifugation was then used to get clear samples for the luminescence study.

Temperature study

The effect of the temperature on the emission properties of the free and encapsulated iridium complexes was examined in this work. To both iridium complex solutions, an excess solid of Q[10] was added in order to prepare the encapsulated samples in a buffer solution. To make these saturated samples clear, centrifugation was used. The temperature of the solutions was controlled using a circulating water bath.

Solvent effect study

For the solvent effect study, iridium complexes (**1** and **2**) were dissolved in different solvents (sodium acetate buffer, methanol, and acetonitrile), and the emission spectra were recorded.

pH effect study

In this experiment, water was used as a solvent. For pH adjustment, diluted aqueous solutions of H$_2$SO$_4$ and NaOH were used for both free complexes and encapsulated species. Encapsulated iridium complex species were prepared by adding an excess of solid Q[10] to a solution of the iridium complexes, followed by centrifugation to obtain clear supernatant solutions.

Stoichiometric and binding studies

The stoichiometry and binding constant of the Q[10] encapsulated complex were obtained using the Benesi–Hildebrand equation.[44] Changes in the absorbance and luminescence intensity upon the addition of Q[10] were used in Benesi–Hildebrand equations. Eqn (2) and (3) for 1 : 1 and 1 : 2 complexes, respectively, are given below:

$$\frac{1}{A - A_0} = \frac{1}{A' - A_0} + \frac{1}{K_a \left(A' - A_0\right)[Q[10]]} \quad (2)$$

$$\frac{1}{A - A_0} = \frac{1}{A' - A_0} + \frac{1}{K_a \left(A' - A_0\right)[Q[10]]^2} \quad (3)$$

$$K_a = \frac{1}{\text{slope} \left(A' - A_0\right)} \quad (4)$$

In the above equations, A_0 (or I_0) is the absorbance (or luminescence intensity) of the guest without Q[10], A (or I) is the absorbance (or emission intensity) with a certain concentration of Q[10], A' (or I') is the absorbance (or emission intensity) at the maximum concentration of Q[10] used and K_a is the binding constant. The linear relation is obtained by plotting $1/(A - A_0)$ *vs.* $1/[Q[10]]$ for 1 : 1 inclusion complexes (eqn (2)) and by plotting $1/A - A_0$ *vs.* $1/[Q[10]]^2$ for 1 : 2 inclusion complexes (eqn (3)). The slope obtained from the Benesi–Hildebrand plot (using eqn (4)) was used to calculate the binding constant K_a.

Density functional theory (DFT)

Gaussian 16, Revision C.02, was used for the DFT calculations. Geometry optimization was performed using the Minnesota functional (M062X) and 6–31+G** basis set for all atoms and LANL2DZ for Ir. The solvation effect (for water) was considered by applying the SMD solvation method.[45] The time-dependent density functional theory (TD-DFT) was used to calculate the UV-visible spectra and corresponding excitation energies.

Iridium complex synthesis

[{Ir(ppy)$_2$μ-Cl}$_2$] was prepared based on the published procedure,[46] and ^{1}H NMR (Fig. S1) was used to confirm the purity of this complex.

[Ir(ppy)$_2$(bpy-(CHO)$_2$)](PF$_6$) (complex 1). This complex was prepared by a method reported by Liu and coworkers[47] with minor modifications in the workup process. In this step and after the reflux, the solvent was evaporated completely; then, the remaining solid was dissolved in water. A saturated aqueous

solution of NH₄PF₆ was added to the previous aqueous solution to produce a red precipitate. The red precipitate was collected by centrifugation and then washed with water and diethyl ether. The precipitate was then dried using a vacuum oven (at 30 °C) to produce pure [Ir(ppy)₂(bpy-(CHO)₂)]PF₆ as a reddish-brown solid.

[Ir(ppy)₂(bpy-(COOH)₂)](PF₆) (complex 2). The complex was prepared using a method reported by Waern and coworkers.[38] The Cl form of this complex was prepared in the same way, but without the last addition of NH₄PF₆. This form was prepared to obtain better solubility in an aqueous medium. The purity of iridium complexes **1** and **2** was confirmed by ¹H NMR (Fig. S2 and S3) and UV-visible (Fig. S4) spectroscopies.

Results and discussion

NMR studies

Different spectroscopic techniques can be used to investigate the supramolecular interactions between host and guest molecules. ¹H NMR is one of the most important methods that is typically used to confirm the formation of the encapsulated species and further gain structural insights. The limited solubility of the resulting encapsulated complexes in aqueous buffer solutions, which falls even below that of the free components, hindered direct measurements using the 400 MHz machine. For this reason, a more sensitive NMR spectrometer (500 MHz) with a different experimental setup (see the SI) was applied to collect evidence of the formation of the encapsulated species of both iridium complexes.

As further support for the encapsulation of complex **1** in the cavity of Q[10], complex **1** and Q[10] were combined in D₂O; however, it was found that the low solubility of **1** retarded the formation of Q[10]·**1**. A comparative spectrum of **1** alone was only feasible if **1** was first dissolved in ACN-d₃ and then diluted with D₂O to a final concentration of 5% ACN-d₃/D₂O (Fig. 2B). It

was also observed that the aldehyde resonance at 10.18 ppm was significantly reduced, indicating partial hydration. Combining **1** and Q[10] in D₂O required extended sonication to form a soluble form of Q[10]·**1**, and the progressive formation was observed by NMR as the free Q[10] doublet resonance at 5.82 ppm decreased and the resonances for the associated guest **1** increased (Fig. 2). The new association product Q[10]·**1** appears as a dynamic multiplex with two new upfield doublets occurring for Q[10] at 5.7 and 5.9 ppm, which suggests two association forms in an approximate ratio of 1:2, respectively. The broadness of the resonances suggests dynamics of different orientations of the guest, possibly between two forms and/or intermediate exchange. The remaining Q[10] resonances (normally a singlet and doublet) fall near the original chemical shift of free Q[10] as broad peaks at 4.2 and 5.5 ppm. Two pertinent guest proton resonances indicate that the phenyl pyridine ligands are located in the cavity and that the bipyridine ligand is near the portal. This is indicated by an upfield shift to 6.2 ppm for the proton doublet α to the Ir–C bond compared to the original shift of 6.4 ppm[38,48] and the downfield shift for the CHO resonance, from 10.2 to 10.3 ppm.

In the case of complex **2**, in the pD range of 2–9, the solubility of Q[10]·**2** is too low for resonances to be visible by ¹H NMR spectroscopy. Adding **2** as a D₂O solution or as a solid to a solution of Q[10] in equimolar quantities results in a yellow precipitate with no resonances observable from the supernatant. When the pD of a suspension of the precipitate in D₂O is adjusted with the addition of NaOD, resonances begin to appear for the free complex **2** and free Q[10] at pD = 8.5, suggesting that the dicarboxylate ion was released. At lower pD < 3.7, **2** must be associated with Q[10] in the protonated form, and above this value, only one carboxylic group would be deprotonated to form a zwitterion complex, with a corresponding increase in the emission. Increasing the pD > 9 results in complete ionisation, and dissociation begins, consistent with the behaviour of carboxylates from Q[7 or 8], as previously reported.[49–57] The ¹H NMR spectrum at pD 9 showed the release of **2** in an excess relative to the observable Q[10] with broader resonances of some of the protons of **2** and the downfield doublet of Q[10], indicating intermediate exchange within the NMR time scale (Fig. 3).
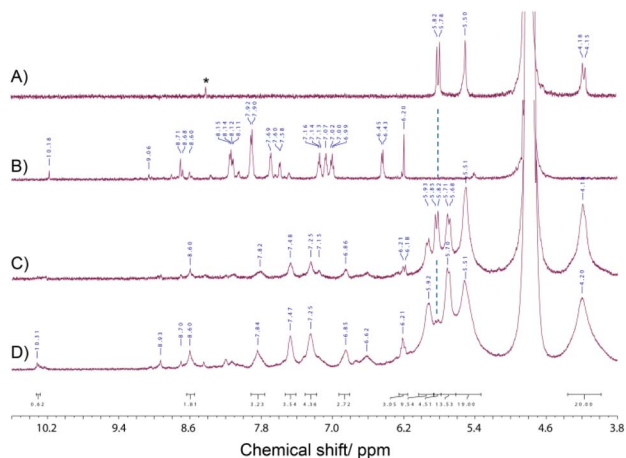

Fig. 2 ¹H NMR spectra (D₂O, 500 MHz) comparing the starting component Q[10] and complex **1** to the formation of the associated complex Q[10]·**1**. (A) Q[10] (* formic acid). (B) Complex **1** dissolved in 5% ACN-d₃/D₂O. (C and D) after the consumption of free Q[10] as the period for sonication was extended.
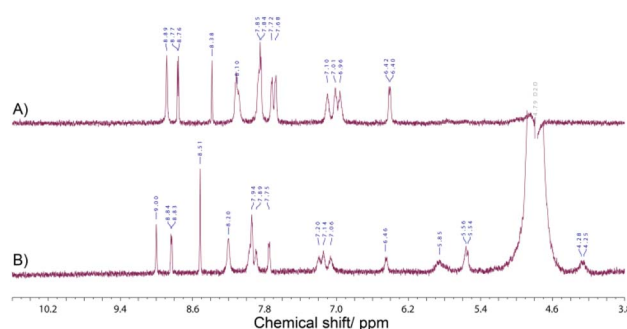

Fig. 3 ¹H NMR spectra (D₂O, 500 MHz) of (A) complex **2** at pD 10 and (B) suspension of Q[10]·**2** in D₂O; pD adjusted with NaOD (0.2 M) to 9.

The luminescent nature of the yellow precipitate obtained in the NMR study was determined in the solid form ($\lambda_{em} = 587$ nm, see the SI). For comparison, equimolar quantities of complex **2** and Q[10] were ground together to a fine homogeneous powder with $\lambda_{em} = 608$ nm. The 2-fold increase in the intensity and the blue shift of 21 nm indicate that the Q[10]·**2** complex is formed almost quantitatively as the yellow precipitate from aqueous solutions (Fig. S12).

Photophysical characterization

The photophysical study was used to emphasize the supramolecular interactions. The sensitivity of UV-visible absorption and luminescence spectroscopies to low concentrations makes them suitable to overcome the low-solubility problem of the encapsulated species. The photophysical data of free complexes and encapsulated species in an aqueous buffer solution are shown in Table 1. The encapsulated species for both complexes were prepared in the presence of excess Q[10], in which the cavity-bound species is dominant (see the binding study).

The absorption spectra of **1** and **2** before and after adding excess Q[10] are shown in Fig. 4. Both complexes display high-energy maxima at 257 and 254 nm, with molar absorptivity (ε) of 4.0×10^4 and 5.0×10^4 M^{-1}cm^{-1}, respectively. These bands can be assigned to the overlapping ^{1}LC ($\pi \rightarrow \pi^*$) transitions of ppy and R-bpy ligands.[58] Fairly intense shoulders appear at 309 and 324 nm, respectively, which are also attributed to the ^{1}LC (possibly ppy) transition.[59] The lower-energy bands (381 and 382 nm for complex **1** and complex **2**, respectively) are assigned to ^{1}LLCT and ^{1}MLCT (from Ir dπ–π^*bpy), respectively.[38,39,59]

Adding Q[10] to the buffer solutions of both complexes (**1** and **2**) has almost similar effects. A minor red shift is noticed with a decrease in the intensity of most absorption bands, especially the high-energy bands ($\lambda_{max} = 257 \rightarrow 260$ nm for **1**, and $\lambda_{max} = 254 \rightarrow 261$ nm for **2**). The bathochromic shift can be related to the alteration in the polarity of the medium (high polar in the buffer to less polar in the host cavity). On the contrary, researchers reported that the absorptivity coefficients of some organic chromophores decrease after encapsulation within Q[n] because the cavity has lower polarizability.[60] The larger shifts of the high-energy bands (^{1}LC), which probably correspond to the ppy ligand,[59] compared to the lowest bands (^{1}MLCT and ^{1}LLCT), may be related to the accommodation mode of these complexes inside Q[10] (see the DFT study). Assuming that the ppy ligand sits inside the cavity, it is
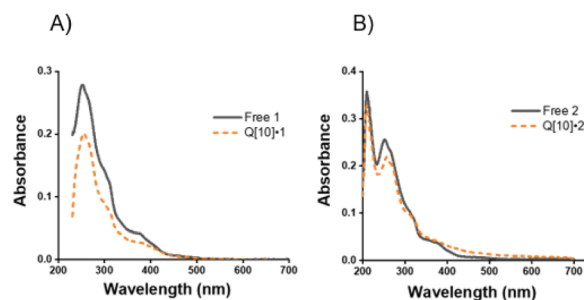

Fig. 4 Absorption spectra of free **1** and the Q[10]·**1** inclusion complex (A) and free **2** and the Q[10]·**2** inclusion complex (B) measured in a buffer solution (pH 4.7) at ambient temperature.

significantly affected by adding Q[10] compared to the bpy ligand, which is located on the portal. This effect is consistent with that observed in our previous study for some iridium complexes[16] and another previous study for polypyridyl ruthenium complexes.[34] TD-DFT calculations were performed to compute the UV-visible spectra of **1** and **2** and their complexes with Q[10]. Despite the slight changes in HOMO–LUMO energy gaps upon the formation of host–guest complexes, the calculated UV-visible spectra nicely reproduce the observed bathochromic shift in λ_{max} upon complexation (see Fig. S8 and Tables S1–S3). The isosurface plots of the HOMO and LUMO wave functions of free **1** and **2** and their Q[10] complexes are given in the SI (Fig. S9 and S10).

In the luminescence study, both **1** and **2** showed broad and weak emission profiles in aqueous buffer solutions. Upon
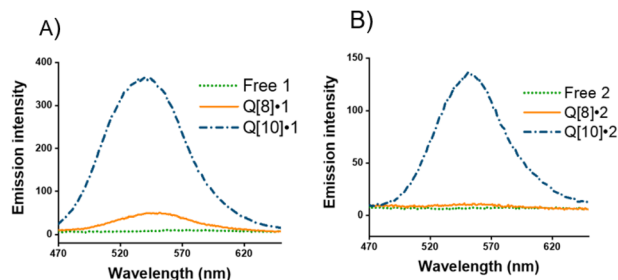

Fig. 5 Luminescence spectra of free **1**, Q[8]·**1** and Q[10]·**1** complexes (A) and free **2**, Q[8]·**2** and Q[10]·**2** (B), measured in a buffer solution (pH 4.7) at room temperature.

Table 1 Photophysical data of the free guests (**1** and **2**) and their complexes with host molecules in a buffer solution (pH 4.7)

	λ_{abs} (nm)	λ_{em} (nm)	Lifetime (ns)	Quantum yield	Enhancement factor	K_a (M^{-1})
1	257 max, 309 sh, 381 sh	575	22	0.014 ± 0.002	—	—
Q[8]·**1**	—	552	279	—	6 times	
Q[10]·**1**	260 max, 312 sh, 388 sh	540	499	0.142 ± 0.016	40 times	1.02×10^6
			93			
2	254 max, 324 sh, 381 sh	578	13	0.023 ± 0.004	—	—
Q[8]·**2**	—	557	27	—	2 times	—
Q[10]·**2**	261 max, 325 sh, 388 sh	553	309	0.060 ± 0.002	20 times	2.31×10^5
			98			

© 2025 The Author(s). Published by the Royal Society of Chemistry

adding Q[10], the emission spectra of Ir-complexes showed a blue shift with a clear enhancement in the emission intensities. The enhancement factors are ~40 times for complex **1** and ~20 times for complex **2** (Fig. 5). This suggests the formation of the encapsulated species (Q[10]·**1** and Q[10]·**2** complexes), which also confirms that the size of the host (portal diameter = ~10.3 Å) is suitable to encapsulate the iridium complexes (~9.6 Å) within its cavity, providing protection to the guest from quenching factors such as solvents and photodegradation.

The quantum yield and lifetime of both complexes are also enhanced after adding Q[10] (Table 1). A biexponential model was required to fit the decay profile obtained from the lifetime measurements, which reveals that the encapsulated systems of both complexes have two different emitting species. For Q[10]·**1**, the long-lived species has a lifetime of 499 ns, while the short-lived species has a lifetime of 93 ns; while in the case of Q[10]·**2**, the lifetime values are 309 and 98 ns for the long-lived and short-lived components, respectively. The short-lived component has a longer lifetime than the free guests (22 ns for complex **1** and 13 ns for complex **2**), suggesting that this system is not a simple 1 : 1 host–guest species but has multiple modes of supramolecular interactions (see the binding study below). This behavior is similar to that noticed in our previous study on other iridium complexes.[16,61]

The enhancement in the luminescence properties of both complexes upon the addition of Q[10] (Table 1) can be attributed to the restricted motion of the iridium guests within the Q[10] cavity, which likely alters the balance between radiative and non-radiative decay pathways by suppressing non-radiative processes. A similar effect was observed on the emission properties of some free iridium complexes upon cooling to 77 K (rigid environment).[62] The blue shift that emission bands display upon adding Q[10] to both complexes can be related to the low polarity of the Q[10] cavity, compared to the aqueous medium. This observation was verified by examining the effect of the solvent polarity on the emission band of unbound **1** and **2**. In both cases, the emission peaks shift to higher energy wavelengths (blue shift) upon moving from a highly polar medium (buffer) to a less polar one (CH$_3$CN) (Fig. S5). This blue shift is mainly related to the destabilization of the ^{3}MLCT excited state in less polar media and will locate close to the ^{3}LC(ppy) state but not above it, which explains the structureless emission profiles of both iridium complexes in the less polar solvent. This result implies that the lowest excited state character is not strongly affected by the solvent polarity. However, the previously studied iridium complexes that have substituent groups on ppy ligands showed structured emission profiles upon encapsulation within Q[10], which suggest that the destabilization of ^{3}MLCT is much stronger in those cases, and the energy of the ^{3}MLCT(bpy) state exceeds the energy of the ^{3}LC state; thus, the emission bands have mainly a ^{3}LC character.[16]

The sensitivity of the luminescence phenomenon of these iridium complexes (**1** and **2**) was also demonstrated by their supramolecular complexation and Q[8], which has a smaller size (portal diameter = 7.3 Å) compared to Q[10]. Exclusion binding is presumed between Q[8] and iridium complexes (9.6 Å diameter). Adding Q[8] to **1** induces a 23 nm blue shift with a 6-fold enhancement in the emission intensity of **1**, while a 21 nm blue shift with an enhancement of 2-fold is observed in the case of **2**. The lifetimes of **1** and **2** are also enhanced upon adding Q[8], and a single exponential is used in the fitting of the emission lifetime, indicating the formation of one emitting species. The structures of the emission bands of both complexes do not change upon adding Q[8], suggesting that the emission bands of host–guest portal binding complexes have the ^{3}MLCT character in both complexes. The blue shift and enhancement that have been displayed in both cases upon portal binding with Q[8] (Fig. 5) can be related to the slight destabilization of the lowest excited state (^{3}MLCT), which is obtained by reducing collisions and the partial protection from the solvent. However, a quenching effect is observed for Q[10] portal binding with ^{3}MLCT emitters, based on the behavior observed for a Ru(II) polypyridyl system.[33]

Binding studies

Luminescence titration experiments were used to estimate the binding affinity of iridium complexes with Q[10]. After adding different volumes of Q[10], the emission intensity of both guests (**1** and **2**) increases significantly with a blue shift (Fig. 6). The shape of the binding curves (Fig. 7) suggests the presence of multiple host–guest emitting species (1 : 1 and 1 : 2), which is in agreement with the non-exponential emission decays noted in the presence of excess Q[10] (based on lifetime measurements). This result is similar to that obtained for previously studied iridium complexes.[61] The modified Benesi–Hildebrand equation was used to calculate the "apparent" binding constant (K_a) of both complexes with the Q[10] host molecule, assuming a 1 : 1 host–guest stoichiometric ratio. The slope and intercept of the double reciprocal plot of $1/(I - I_0)$ *vs.* $1/[\text{Q}[10]]$ were used to get the K_a values. For a higher order of complexation complexes, this fitting would be nonlinear. The obtained K_a values are 1.02×10^6 and 2.31×10^5 M^{-1} for complexes **1** and **2**, respectively (Fig. 7).

The binding constants of iridium complexes with Q[10] were also estimated using the UV-visible spectroscopic technique. Absorption titration experiments were carried out for each complex with Q[10] in a buffer solution. A decrease in the absorbance values of each iridium complex with a small red shift resulted after Q[10] addition (Fig. S6). The modified
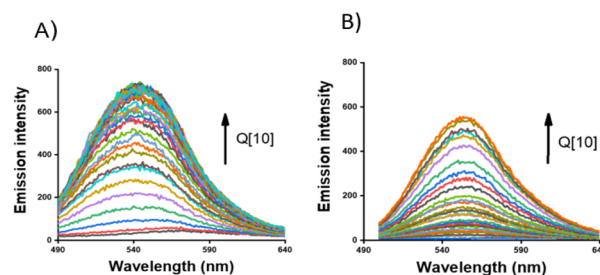

Fig. 6 Luminescence titration spectra of **1** (5.9×10^{-6} M) (A) and **2** (7.6×10^{-7} M) (B) in the presence of different concentrations of Q[10], in a buffer solution (pH 4.7) at ambient temperature.
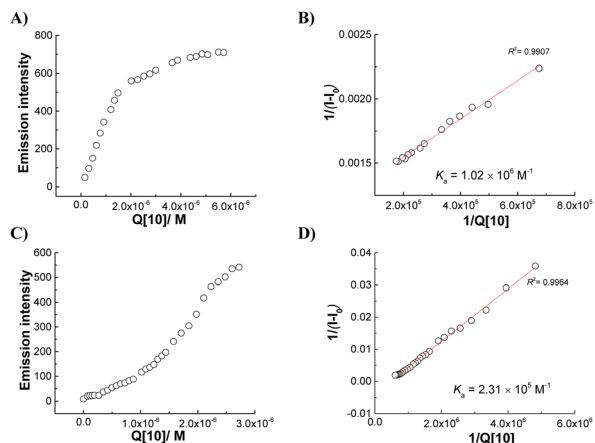
Fig. 7 (A and C) Luminescence binding curves of iridium complexes **1** (λ_{em} = 540 nm) and **2** (λ_{em} = 553 nm), respectively, as a function of the Q[10] concentration in a buffer (pH 4.7) at ambient temperature. (B and D) Benesi–Hildebrand plots of both complexes over the high Q[10] portion of the curve (demonstrating a 1 : 1 host–guest binding mode).

Fig. 9 Schematic illustrating the effect of temperature on the binding equilibrium between emitting species.

Benesi–Hildebrand equation was also used to determine the binding constants K_a of both complexes with Q[10], assuming a 1 : 1 host–guest stoichiometric ratio. The estimated binding constants are found to be 2.6×10^6 M^{-1} for complex **1** and 6.3×10^5 M^{-1} for complex **2** (Fig. S7), which are in good agreement with the values obtained by luminescence titrations. The lower K_a value of complex **2** compared to complex **1** may be related to the repulsion force between the carboxylate moiety COO$^-$ and the portal carbonyl groups of the host molecule[49,51] (see the pH study below).

Temperature study

The sensitivity of the emission profile of the free iridium complexes and their host–guest assemblies was investigated in this study. Upon changing the temperature from 15 to 55 °C, a clear decrease in the emission intensity of both encapsulated species (Q[10]·**1** and Q[10]·**2**) is noticed (Fig. 8), in agreement with previously published work.[16] This result shows that the temperature has a significant impact on the binding equilibrium: elevating the temperature reduces the amount of the strongly emissive cavity-bound species (1 : 1 host–guest) and shifts the equilibrium to 1 : 1 or 1 : 2 portal-bound forms or the free species (Fig. 9). In the last status, a clear change in the
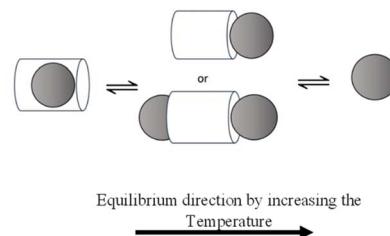
emission peaks is unlikely to be seen, as these emitting species are very weak compared to the strong 1 : 1 encapsulated species. The emission profile can be quenched by increasing the temperature as a result of the activation of non-radiative pathways (collisions and vibrations). Applying the same study to both free complex **1** and complex **2** gave an insignificant change in the emission intensity. In general, emitting species that possess long lifetimes are usually more sensitive to the temperature than those that possess short lifetimes. Thus, the impact of the temperature on the emission profile is probably a result of its influence on the binding equilibrium and non-radiative pathways together.

pH study

The effect of pH variation on the emission spectra of both free and Q[10]-encapsulated iridium complexes (**1** and **2**) was also investigated. Expectedly, no change is observed for both free and encapsulated complex **1**, while a significant effect is observed in the case of complex **2** because of the presence of carboxylic acid groups on the bpy ligand. By increasing the pH from 2 to 10, the emission spectra of both free complex **2** and Q[10]·**2** shift to higher energies (blue shift). This shift is strong for free **2** (585 → 570 nm) but weaker in the case of Q[10]·**2** (558 → 554 nm). An increase in the emission intensity is observed upon increasing the pH for both the free and encapsulated species (Fig. S11), suggesting that the Ir–COO$^-$ form (under highly basic conditions) is a stronger emitting species than the protonated form Ir–COOH.[51] The encapsulation process of ionizable guest molecules within Q[n] can result in a shift in their pK_a values.[16,34] The emission response of free **2** as a function of the pH reveals a single inflection point, with an
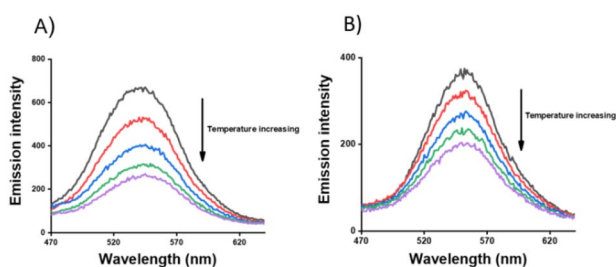

Fig. 8 Luminescence spectra of Q[10]·**1** (A) and Q[10]·**2** (B) in a buffer solution (pH 4.7) at different temperature (15–55 °C).
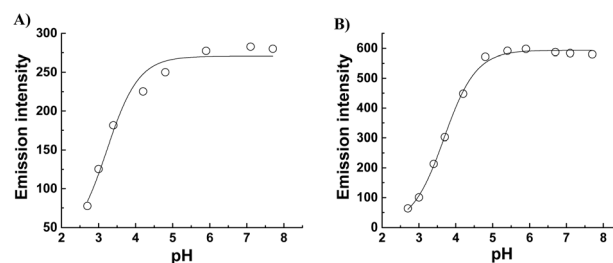

Fig. 10 Emission intensity plot for (A) unbound **2** at 584 nm and (B) encapsulated species Q[10]·**2** at 553 nm as a function of pH at ambient temperature.

excited-state pK_a value (pK_a*) of 3.21 ± 0.20. It is worth noting that the acid–base behavior of similar complexes was previously investigated.[63,64] For example, ruthenium(II) complexes containing dicarboxybipyridine [Ru(bpy)$_2$(bpy-(COOH)$_2$)] show two closely ground-state pK_a values of 1.75 and 2.85 and a single excited-state pK_a* of 4.25.[63] The pK_a* value of the encapsulated species Q[10]·**2** is measured to be 3.68 ± 0.03 (Fig. 10). This pK_a shift (ΔpK_a ~0.5) reveals that the proton of COOH is less acidic in the encapsulated form due to the favorable interaction of the COOH with the portal of Q[10].[49,51] It should be noted that the second deprotonation equilibrium is observed at a pH above 9.

Density functional theory (DFT)

The free Q[10] and iridium cyclometalated complexes were optimized in water by the M062X method and 6–31+G** basis set for all atoms and LANL2DZ for Ir. As shown in Fig. 11, the Q[10] structure is symmetrical with cavity and portal diameters of ~11 and 10 Å,[65] respectively, which is sufficiently large to accommodate the iridium complexes (**1** and **2**).
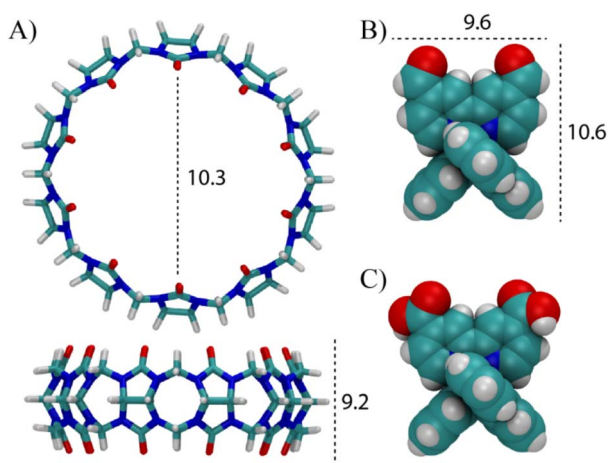

Fig. 11 DFT–optimized structures (M062X/6–31+G**/LANL2DZ, in water) of (A) free Q[10] and iridium cyclometalated complexes (B) complex **1** (R = −CHO), and (C) complex **2** (R = −COOH). Distances are given in Å.
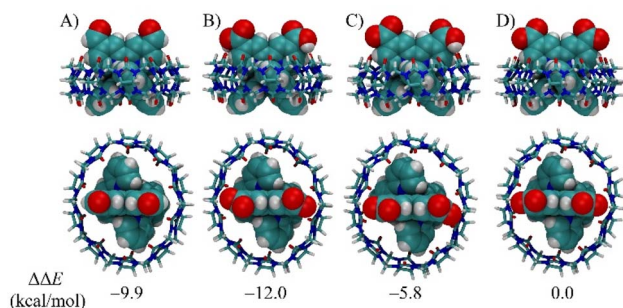

Fig. 12 DFT-optimized structures (M062X/6–31+G**/LANL2DZ, in water) of Q[10]-iridium cyclometalated complexes: (A) Q[10]·**1** (R = −CHO), (B) Q[10]·**2** (R = −COOH), (C) Q[10]·**2** (R = −COOH/−COO⁻), and (D) Q[10]·**2** (R = −COO⁻).

The optimized structures of the Q[10]-complexes are shown in Fig. 12. The substituted iridium cyclometalated complexes show similar binding modes, in which they all fit well inside the cavity of Q[10]. As expected, the hydrophobic part is deeply encapsulated inside the inner cavity, while the hydrophilic groups (–CHO, –COOH, and –COO⁻) are excluded and more exposed to water. In the case of the protonated carboxylated iridium complex (Ir–COOH), the complex is further stabilized by hydrogen bonding with the carbonyl portal of Q[10] with a hydrogen bond distance of 1.7 Å. The calculated binding energy reveals higher affinity for Q[10]·**2** (R = −CO$_2$H), followed by Q[10]·**2** (R = −CHO). It should be noted that the weak binding affinity of the dicarboxylated complex **2** is in accordance with its dissociation from the cavity, as seen in ¹H NMR experiments (Fig. 3).

Conclusions

Iridium complexes (complex **1** and complex **2**) that have different substituent groups on the bipyridine ligand can be encapsulated within the Q[10] cavity in an aqueous solution. The encapsulation of both iridium complexes in Q[10] reveals the significant effect on their luminescence properties, quantum yields and lifetimes, offering an alternative to traditional ligand modification for tuning emission colors. In addition, the pH study reveals the complexation-induced pK_a shift of complex **2**. This study demonstrates that changing the position of the substituent groups from the ppy ligand (as in our previous work) to the bpy ligand (in the current study) does not significantly affect the binding mode of the iridium complexes within Q[10]. This strategy holds significant promise for applications reliant on the luminescent properties of such complexes, particularly in sensing. Furthermore, because the bipyridine (bpy) ligand extends outside the Q[10] cavity, it remains accessible for functionalization (e.g., with CHO or COOH groups), enabling interactions with analytes such as amino acids without disrupting the host–guest complex. This structural feature makes the system well-suited for the development of responsive, water-compatible luminescent sensors, including biosensors. Finally, the contrast in the solubility of CHO complex **1** and (–COOH)$_2$ complex **2** when encapsulating them in Q[10] is important to understand when developing potential applications. Increasing solubility in an aqueous environment has sensing potential in environmental chemistry and/or biochemistry. The low solubility and ease of formation of Q[10]·**2** and the zwitterion may make this association complex and similar construction applicable to the development of electronic devices.

Conflicts of interest

There are no conflicts to declare.

Data availability

Acknowledgements

Notes and references

1 D. L. Ma, S. Lin, W. Wang, C. Yang and C. H. Leung, *Chem. Sci.*, 2017, **8**, 878–889.

2 Q. bo Mei, L. Liu, J. chang Yang, S. hui Ye and B. hai Tong, *Dyes Pigm.*, 2021, **191**, 109360.

3 S. Ladouceur, K. N. Swanick, S. Gallagher-Duval, Z. Ding and E. Zysman-Colman, *Eur. J. Inorg. Chem.*, 2013, 5329–5343.

4 N. D. McDaniel, F. J. Coughlin, L. L. Tinker and S. Bernhard, *J. Am. Chem. Soc.*, 2008, **130**, 210–217.

5 M. Palmese, J. J. Pérez-Torrente and V. Passarelli, *Dalton Trans.*, 2022, **51**, 12334–12351.

6 A. A. Eremina, M. A. Kinzhalov, E. A. Katlenok, A. S. Smirnov, E. V. Andrusenko, E. A. Pidko, V. V. Suslonov and K. V. Luzyanin, *Inorg. Chem.*, 2020, **59**, 2209–2222.

7 W. Wang, C. Wu, C. Yang, G. Li, Q. Bin Han, S. Li, S. M. Y. Lee, C. H. Leung and D. L. Ma, *Sens. Actuators, B*, 2018, **255**, 1953–1959.

8 Z. Yan, J. Wang, Y. Zhang, S. Zhang, J. Qiao and X. Zhang, *Chem. Commun.*, 2018, **54**, 9027–9030.

9 Q. Wu, K. Y. Zhang, P. Dai, H. Zhu, Y. Wang, L. Song, L. Wang, S. Liu, Q. Zhao and W. Huang, *J. Am. Chem. Soc.*, 2020, **142**, 1057–1064.

10 A. Y. Zakharov, I. V. Kovalenko, E. A. Meshcheriakova, E. V. Nykhrikova, A. O. Zharova, M. A. Kiseleva, P. Kalle, E. V. Tekshina, S. A. Kozyukhin, V. V. Emets and S. I. Bezzubov, *Russ. J. Coord. Chem.*, 2022, **48**, 846–858.

11 F. Monti, A. Baschieri, L. Sambri and N. Armaroli, *Acc. Chem. Res.*, 2021, **54**, 1492–1505.

12 Y. Tang, H. R. Yang, H. Bin Sun, S. J. Liu, J. X. Wang, Q. Zhao, X. M. Liu, W. J. Xu, S. B. Li and W. Huang, *Chem.–Eur. J.*, 2013, **19**, 1311–1319.

13 L. Xiong, Q. Zhao, H. Chen, Y. Wu, Z. Dong, Z. Zhou and F. Li, *Inorg. Chem.*, 2010, **49**, 6402–6408.

14 Y. Ma, S. Liu, H. Yang, Y. Wu, H. Sun, J. Wang, Q. Zhao, F. Li and W. Huang, *J. Mater. Chem. B*, 2013, **1**, 319–329.

15 M. J. Li, P. Jiao, M. Lin, W. He, G. N. Chen and X. Chen, *Analyst*, 2011, **136**, 205–210.

16 L. R. Alrawashdeh, M. P. Cronin, C. E. Woodward, A. I. Day and L. Wallace, *Inorg. Chem.*, 2016, **55**, 6759–6769.

17 E. Masson, X. Ling, R. Joseph, L. Kyeremeh-Mensah and X. Lu, *RSC Adv.*, 2012, **2**, 1213–1247.

18 X. Yang, F. Liu, Z. Zhao, F. Liang, H. Zhang and S. Liu, *Chin. Chem. Lett.*, 2018, **29**, 1560–1566.

19 A. L. Koner and W. M. Nau, *Supramol. Chem.*, 2007, **19**, 55–66.

20 S. Zhang, L. Grimm, Z. Miskolczy, L. Biczók, F. Biedermann and W. M. Nau, *Chem. Commun.*, 2019, **55**, 14131–14134.

21 S. Liu, C. Ruspic, P. Mukhopadhyay, S. Chakrabarti, P. Y. Zavalij and L. Isaacs, *J. Am. Chem. Soc.*, 2005, **127**, 15959–15967.

22 Q. Duan, R. Chen, S. Deng, C. Yang, X. Ji, G. Qi, H. Li, X. Li, S. Chen, M. Lou and K. Lu, *Front. Chem.*, 2023, **11**, 1–5.

23 Y. Zhang, G. Zhang, X. Xiao, Q. Li and Z. Tao, *Coord. Chem. Rev.*, 2024, **514**, 215889.

24 S. J. Barrow, S. Kasera, M. J. Rowland, J. Del Barrio and O. A. Scherman, *Chem. Rev.*, 2015, **115**, 12320–12406.

25 B. Al Tbakhi, H. Nsairat, W. Alshaer, A. Al-Kadash, W. Helal, L. Alrawashdeh, A. Day, K. I. Assaf, R. Hassouneh, F. Odeh and A. Al Bawab, *RSC Adv.*, 2022, **12**, 7540–7549.

26 L. Alrawashdeh, K. I. Assaf, W. Alshaer, F. Odeh and S. A. Bani-Atta, *RSC Adv.*, 2022, **12**, 1982–1988.

27 L. Alrawashdeh, B. F. Kulaib, K. I. Assaf, M. I. El-Barghouthi, K. Bodoor, O. M. Abuhasan and A. A. Abdoh, *J. Mol. Liq.*, 2023, **380**.

28 S. Liu, P. Y. Zavalij and L. Isaacs, *J. Am. Chem. Soc.*, 2005, **127**, 16798–16799.

29 Q. Li, S. C. Qiu, J. Zhang, K. Chen, Y. Huang, X. Xiao, Y. Zhang, F. Li, Y. Q. Zhang, S. F. Xue, Q. J. Zhu, Z. Tao, L. F. Lindoy and G. Wei, *Org. Lett.*, 2016, **18**, 4020–4023.

30 X. Cheng, L. Liang, K. Chen, N. Ji, X. Xiao, J. Zhang, Y. Zhang, S. Xue, Q. Zhu, X. Ni and Z. Tao, *Angew. Chem., Int. Ed.*, 2013, **52**, 7252–7255.

31 S. Liu, A. D. Shukla, S. Gadde, B. D. Wagner, A. E. Kaifer and L. Isaacs, *Angew. Chem., Int. Ed.*, 2008, **47**, 2657–2660.

32 W. Gong, X. Yang, P. Y. Zavalij, L. Isaacs, Z. Zhao and S. Liu, *Chem.–Eur. J.*, 2016, **22**, 17612–17618.

33 M. J. Pisani, Y. Zhao, L. Wallace, C. E. Woodward, F. R. Keene, A. I. Day and J. G. Collins, *Dalton Trans.*, 2010, **39**, 2078–2086.

34 E. T. Luis, A. I. Day, B. König and J. E. Beves, *Inorg. Chem.*, 2020, **59**, 9135–9142.

35 K. M. Anis-Ul-Haque, C. E. Woodward, A. I. Day and L. Wallace, *Inorg. Chem.*, 2020, **59**, 3942–3953.

36 R. N. Dsouza, U. Pischel and W. M. Nau, *Chem. Rev.*, 2011, **111**, 7941–7980.

37 L. R. Alrawashdeh, A. I. Day and L. Wallace, *Dalton Trans.*, 2013, **42**, 16478–16481.

38 J. B. Waern, C. Desmarets, L. M. Chamoreau, H. Amouri, A. Barbieri, C. Sabatini, B. Ventura and F. Barigelletti, *Inorg. Chem.*, 2008, **47**, 3340–3348.

39 B. Das, S. T. Borah, S. Ganguli and P. Gupta, *Chem.–Eur. J.*, 2020, **26**, 14987–14995.

40 J. Kim, I. S. Jung, S. Y. Kim, E. Lee, J. K. Kang, S. Sakamoto, K. Yamaguchi and K. Kim, *J. Am. Chem. Soc.*, 2000, **122**, 540–541.

41 S. Liu, P. Y. Zavalij and L. Isaacs, *J. Am. Chem. Soc.*, 2005, **127**, 16798–16799.

42 J. N. Demas and G. A. Crosby, *J. Phys. Chem.*, 1971, **75**, 991–1024.

43 J. Jayaraju, K. C. Basavaraju, J. Keshavayya and S. K. Rai, *J. Macromol. Sci., Part B: Phys.*, 2006, **45**, 741–751.

44 N. Saleh and N. A. F. Al-Rawashdeh, *J. Fluoresc.*, 2006, **16**, 487–493.

45 A. V. Marenich, C. J. Cramer and D. G. Truhlar, *J. Phys. Chem. B*, 2009, **113**, 6378–6396.

46 S. Sprouse, K. A. King, P. J. Spellane and R. J. Watts, *J. Am. Chem. Soc.*, 1984, **106**, 6647–6653.

47 J. B. Liu, C. Yang, C. N. Ko, K. Vellaisamy, B. Yang, M. Y. Lee, C. H. Leung and D. L. Ma, *Sens. Actuators, B*, 2017, **243**, 971–976.

48 F. Scarpelli, A. Ionescu, L. Ricciardi, P. Plastina, I. Aiello, M. La Deda, A. Crispini, M. Ghedini and N. Godbert, *Dalton Trans.*, 2016, **45**, 17264–17273.

49 W. S. Jeon, K. Moon, S. H. Park, H. Chun, Y. H. Ko, J. Y. Lee, E. S. Lee, S. Samal, N. Selvapalam, M. V. Rekharsky, V. Sindelar, D. Sobransingh, Y. Inoue, A. E. Kaifer and K. Kim, *J. Am. Chem. Soc.*, 2005, **127**, 12984–12989.

50 L. Yuan, R. Wang and D. H. Macartney, *Tetrahedron:Asymmetry*, 2007, **18**, 483–487.

51 O. Buyukcakir, F. T. Yasar, O. A. Bozdemir, B. Icli and E. U. Akkaya, *Org. Lett.*, 2013, **15**, 1012–1015.

52 V. Sindelar, S. Silvi and A. E. Kaifer, *Chem. Commun.*, 2006, 2185–2187.

53 A. E. Kaifer, W. Li, S. Silvi and V. Sindelar, *Chem. Commun.*, 2012, **48**, 6693–6695.

54 L. Lei, L. Luo, X. L. Wu, G. H. Liao, L. Z. Wu and C. H. Tung, *Tetrahedron Lett.*, 2008, **49**, 1502–1505.

55 H. J. Buschmann, L. Mutihac and E. Schollmeyer, *J. Inclusion Phenom. Macrocyclic Chem.*, 2006, **56**, 363–368.

56 V. Kolman, P. Kulhanek and V. Sindelar, *Chem.–Asian J*, 2010, **5**, 2386–2392.

57 A. R. Urbach and V. Ramalingam, *Isr. J. Chem.*, 2011, **51**, 664–678.

58 S. I. Bokarev, O. S. Bokareva and O. Kühn, *J. Chem. Phys.*, 2012, **136**(21), 214305.

59 S. H. Wu, J. W. Ling, S. H. Lai, M. J. Huang, C. H. Cheng and I. C. Chen, *J. Phys. Chem. A*, 2010, **114**, 10339–10344.

60 W. M. Nau, M. Florea and K. I. Assaf, *Isr. J. Chem.*, 2011, **51**, 559–577.

61 L. R. Alrawashdeh, M. P. Cronin, A. I. Day, L. Wallace and C. E. Woodward, *Analyst*, 2018, **143**, 519–527.

62 K. K. Lo, K. Y. Zhang, S. Leung and M. Tang, *Angew. Chem., Int. Ed.*, 2008, **47**, 2213–2216.

63 M. K. Nazeeruddin and K. Kalyanasundaram, *Inorg. Chem.*, 1989, **28**, 4251–4259.

64 M. K. Nazeeruddin, S. M. Zakeeruddin, R. Humphry-Baker, M. Jirousek, P. Liska, N. Vlachopoulos, V. Shklover, C. H. Fischer and M. Grätzel, *Inorg. Chem.*, 1999, **38**, 6298–6305.

65 A. I. Day, R. J. Blanch, A. P. Arnold, S. Lorenzo, G. R. Lewis and I. Dance, *Angew. Chem., Int. Ed.*, 2002, **41**, 275–277.